Journal of Taibah University for Science

ISSN: (Print) (Online) Journal homepage: https://www.tandfonline.com/loi/tusc20

Effects of Rashba spin–orbit interaction and topological defect on the magnetic properties of an electron confined in a 2D quantum dot

Nouf Ibrahim, Muayad Abu Saa, Ayham Shaer & Mohammad Elsaid

To cite this article: Nouf Ibrahim, Muayad Abu Saa, Ayham Shaer & Mohammad Elsaid (2021) Effects of Rashba spin–orbit interaction and topological defect on the magnetic properties of an electron confined in a 2D quantum dot, Journal of Taibah University for Science, 15:1, 1210-1216, DOI: 10.1080/16583655.2022.2025691

To link to this article: https://doi.org/10.1080/16583655.2022.2025691

Published online: 23 Jan 2022.

JOURNAL OF TAIBAH UNIVERSITY FOR SCIENCE
2021, VOL. 15, NO. 1, 1210–1216
https://doi.org/10.1080/16583655.2022.2025691

JTUSCI

Journal of Taibah University for Science

Taylor & Francis
Taylor & Francis Group

RESEARCH ARTICLE

OPEN ACCESS Check for updates

Effects of Rashba spin–orbit interaction and topological defect on the magnetic properties of an electron confined in a 2D quantum dot

Nouf Ibrahim [a], Muayad Abu Saa [a], Ayham Shaer [b] and Mohammad Elsaid [b]

[a]Faculty of Science, Physics Department, Arab American University, Jenin, Palestine; [b]Faculty of Science, Physics Department, An-Najah National University, Nablus, Palestine

ABSTRACT

The energy spectra of Hamiltonian of a single electron confined in a parabolic quantum dot (QD) have been investigated, taking into considerations different external effects such as the Rashba spin–orbit interaction term, applied uniform magnetic field and topological defect. The results show that the topological defect enhances the energy levels, while the increment in the strength of Rashba parameter removes the spin degeneracy and reduces the energy levels. The obtained QD energy spectra are used to study the statistical mean energy from which we consider the behaviour of the magnetization and magnetic susceptibility on the QD. It is found that the topological defects and Rashba terms play important roles in flipping the sign of the magnetic susceptibility from negative ($\chi < 0$) to positive sign ($\chi > 0$). The present results are in very good qualitative agreement compared with the reported ones.

ARTICLE HISTORY
Received 8 March 2021
Revised 6 October 2021
Accepted 29 December 2021

KEYWORDS
Quantum dot; Rashba effect; topological defect; magnetization and magnetic susceptibility; magnetic phase diagram

1. Introduction

Quantum dot (QD) is a nanostructured material that confined the carriers in all three directions, reducing the degrees of freedom to zero and exhibiting a discrete energy spectrum, as in a natural atom [1–3]. The addition of a magnetic field and Rashba term will make the Hamiltonian problem very interesting research problem in the field of nanoscience and technology. Semiconductor nanostructure QDs have become very hot research subject due to their potential device applications such as QD lasers, quantum computation, QD solar cells, biological and medical application such as the image cancer treatment [4–6]. The spin–orbit coupling phenomena in semiconductor QDs system is very important interaction energy term as it plays an essential role in controlling the properties of the QD which makes the QD an excellent basis in the new emerging field of technology, called spintronics. The QD-spin transistor is considered to be an important electronic device in the area of spintronics. Different authors had, very recently, studied the thermodynamic and magnetic properties of the QD systems in the presence of a magnetic field [7,8]. Baghdasaryan et al. [7] had considered the thermal and magnetic properties of an electron confined in a toroidal QD in the presence of an applied magnetic field. Sedehi and Khordad had presented a theoretical study on the magnetic and thermal properties of QD/ring with different potentials: parabolic-inverse confinement potential and modified Gaussian potential under the effect of an applied uniform magnetic field [9]. Edet et al. had investigated the position-dependent mass Schrodinger equation for the screened potential with Aharanov–Bohm (AB) and external magnetic field. The thermodynamic properties and magnetic susceptibility of the system at various temperature range had been studied [10]. The combined effects of pressure, and the spin–orbit interaction on the QD energy spectra had also been considered [11,12].

In this work, we studied, in detail, the combined effects, both topological defects and the spin–orbit interaction term on the properties of the QD. We consider a single electron QD confined in two dimensions in the presence of a magnetic field, taken to be along *z*-axis, in addition to the spin–orbit interaction term. The total Hamiltonian of QD system is solved and the corresponding energy spectra are obtained in analytical form. The obtained energies are used to calculate the partition functions and investigate the variation of the energy levels, magnetic and thermal properties of the zero-dimensional semiconductor QD systems with the presence of Rashba and topological effect terms. We display the significance of the topological defect and Rashba strength in the change of the magnetic phase of the QD-material from diamagnetic to paramagnetic

CONTACT Muayad Abu Saa muayad.abusaa@aaup.edu

type and the flip in the sign of magnetic susceptibility (χ) from negative (−) to positive (+). The rest of this work is organized as follows. The Hamiltonian of a single electron confined in a QD, taking into consideration the combined effects of Rashba spin–orbit interaction and topological defect, are presented in the theory- part. We have displayed the computed numerical results of the magnetic quantities in results and discussion- part. Our conclusions are given in the final part.

2. Theory

The Hamiltonian of an electron confined in QD by a potential, $V_c(r)$, and under the effect of an applied uniform magnetic field and spin–orbit interaction term can be given as

$$\hat{H} = \frac{1}{2m*}\left[\vec{P} + \frac{e}{c}\vec{A}\right]^2 + V_c(r) + H_R \tag{1}$$

where m^* is the electron effective mass of the material of GaAs QDs, $\vec{P}$ refers to the electron momentum operator, e is the elementary charge, c is the speed of light,

$\vec{A}$ is the vector potential is chosen to be in the symmetric gauge as

$$A = \frac{B}{2}(-y, x, 0) \tag{2}$$

$V_c(r)$ is the confining potential, modelled as a parabolic-type-like,

$$V_c(r) = \frac{1}{2}m^*\omega_0^2 r^2, \tag{3}$$

where ω_0 is the strength of the confinement potential frequency,

r is the position vector of an electron in the QD and its equal $(x^2 + y^2)^{\frac{1}{2}}$,

$$H_R = \alpha_R \overrightarrow{\sigma}.\left[\vec{\nabla}V(r) \times \left(\vec{p} - \frac{e}{c}A\right)\right]/h \tag{4}$$

where H_R is the Rashba term, α_R is the Rashba parameter strength of SOI, σ are the Pauli matrices, $\{\sigma_x, \sigma_y\}$, ħ is Plank's constant [13,14].

Topological effect is the surface of the QD which has a topological defect described in polar coordinates (ρ, φ) by the metric [15]:

$$dl^2 = d\rho^2 + \rho^2 d\varphi^2 \tag{5}$$

where $\rho = \alpha^{-1}r, \varphi = \alpha\theta$, then the metric becomes

$$dl^2 = \alpha^{-2}dr^2 + r^2 d\theta^2 \tag{6}$$

while α is a kink parameter and it controls the cut off, whereas $0 < \alpha < 1$, if $\alpha = 1$ means that there is no effect of topological defect, with φ belongs to $0 < \varphi < 2\pi\alpha$, and $0 < \theta < 2\pi$.

The total QD Hamiltonian, H, can be reduced to a solvable harmonic oscillator one with analytical energy spectra expression. The eigen energy spectra are defined, in terms of the quantum numbers (n, l) and other physical functions [15], as

$$E_{n,l,s}(\omega_0, \omega_c, \gamma, p) = \hbar\Omega(2n + p|l| + 1) + \frac{p^2}{2}\hbar\omega_c l + \left(\gamma m^* {\omega_0}^2 l + \frac{1}{4}g^*\hbar\omega_c\right)s \tag{7}$$

where Ω is the effective frequency and defined as

$$\Omega^2 = \left(1 + s\gamma\frac{m * \omega_c}{\hbar}\right){\omega_0}^2 + \left(\frac{\omega_c p}{2}\right)^2 \tag{8}$$

$$\omega_c = \frac{eB}{m^* c} \tag{9}$$

ω_c denotes the cyclotron frequency, s is the spin of the electron, γ is the Rashba spin orbit parameter, p is the topological parameter and it equal the inverse of kink parameter (α^{-1}), $n = 0, 1, 2, \ldots$. is the radial quantum number, $l = 0, \pm1, \pm2, \ldots$, is the angular quantum number and g^* is the effective Lande g-factor.

The obtained eigen energies of the QDs will be used as input essential data to calculate the statistical average energy,

$$\langle E_{n.l,s}(\omega_0, \omega_c, \gamma, p)\rangle = \frac{\sum_{\alpha=1}^{i} E_\alpha e^{-\beta E_\alpha}}{\sum_{\alpha=1}^{i} e^{-\beta E_\alpha}} \tag{10}$$

where $\beta = \frac{1}{k_B T}$ and k_B is the Boltzmann constant. Having computed the average energy, all the thermal and magnetic quantities of the QD can be obtained using the well-known relations: Magnetization [13,14,16],

$$M = -\frac{\partial\langle E_{n.l,s}(\omega_0, \omega_c, \gamma, p)\rangle}{\partial B} \tag{11}$$

and Magnetic Susceptibility,

$$\chi = \frac{\partial \mathrm{M}}{\partial \mathrm{B}}. \tag{12}$$

The dependence of the thermal and magnetic functions will be investigated as functions of confinement strength, magnetic field cyclotron frequency, Rashba term, topological factor and temperature. In addition, the phase diagram for the magnetic susceptibility will be plotted as function of topological defect, Rashba term, magnetic field strength and temperature to show the magnetic transition of the GaAs from diamagnetic to paramagnetic.

3. Results and discussion

In this section, we discuss the obtained results for the energy spectra of an electron confined in a parabolic QD in presence of RSOI term, topological effect and an applied uniform magnetic field. We study the physical properties of the GaAs QDs material by computing the statistical energy, magnetization and susceptibility. For GaAs QD, we used the following physical parameters; effective electron mass: $m^* = 0.067m_e$,

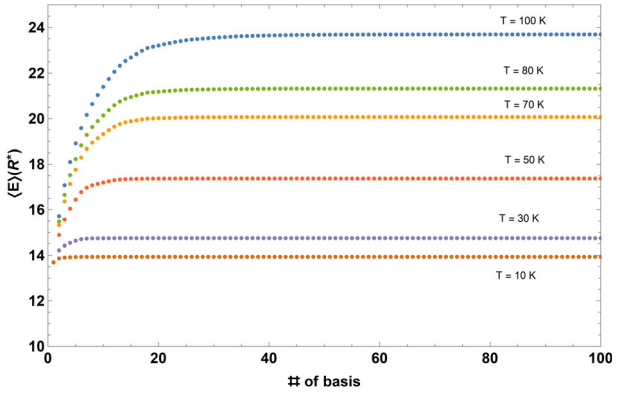

Figure 1. The $\langle E\rangle$ versus # of bases with different temperature (T) range, from 10 K to 100 K, T at $\omega_c = 3\,R*, \omega_0 = 2.5\,R*, \gamma = 0.5a^*.R^*$ and $p = 1$.

effective Lande factor: $g* = -0.44$, effective Rydberg energy:$R^* = 5.694$ meV, effective Bohr radius: $a^* = 9.8$ nm, Rashba parameter $\gamma(1a^*.R^* = 55.8$ meV.nm) and magnetic field ω_c ($\omega_c(R*) = 0.296 \times (B$ in Tesla $(T))$.

In Figure 1, as a significant convergency test to our computational scheme, we have displayed the calculated average energies against the number of basis (#) for different temperature range, from 10 K to 100 K, and physical QD functions. As the energy of the QD-system increases, the electron average energy $\langle E\rangle$ enhances due to the available thermal energy, $E_{th} \approx k_bT$, which is gained by the electron as an excitation energy. The average energy plot clearly shows a numerical stability for various values of Hamiltonian functions. Based on the following two important issues, first, the energy spectra ($E_{n,l,s}$) expression is an exact one, given by Equation (7), second, the present convergency test for the average energy $< E >$ will produce accurate computed numerical results for magnetic (M) and susceptibility (χ) quantities.

In Figure 2(a), we have used equation (7) to plot the QD Fock-Darwin states as a function of a magnetic field strength for $p = 1, \omega_0 = 2.5\,R*$ and zero Rashba parameter $\gamma = 0$.The energy spectra show a similar behaviour with the corresponding ones given by Ref. [14], The labeled of the Fock-Darwin energy states $|n, l, s\rangle$ were plotted in Figure 2(a) from the bottom at $\omega_c = 1R^*$ are: $|0, 0, +\rangle$, $|0, 0, -\rangle$, $|0, -1, +\rangle$, $|0, -1, -\rangle$, $|0, 1, +\rangle$ and $|0, 1, -\rangle$. The plot clearly shows that a converging average energy value can be obtained for small number of bases ≈ 20, at low temperature, while at high temperature, we need around 40 bases.

Figure 2(c) displays the effect of topological defect (p) on the QD energy spectra, we observe that the energy state increases at constant ω_c for spin up and down. For $l = 0$ and 1, the energy level increases as ω_c increases, while the energy decreases for the case of $l = -1$ at $\omega_c = 3R^*$ and then increases, it is attributed to the electron confinement in a small region which leads to an enhancement in the momentum, and in turn the kinetic energy, by uncertainty principle [13] and eventually the energy of the electron increases. In Figure 2(d), the Rashba effect removes the spin degeneracy for $l = +1$ and $l = -1$ energy states by showing wide energy splitting, ΔE, for spin up and spin down states.

The behaviour of the energy spectra due to the Rashba and topological effects are shown in Figure 2(d).

To investigate the effects of external parameters such as Rashba and topological defect on the energy levels of the QD, we have plotted in Figure 3 $< E >$ against ω_c for $\omega_0 = 2.5\,R*$ and various selected values of temperature.

If we apply, jointly, RSOI and p as in Figure 3(d), the effect of γ is higher than p until $\omega_c \approx 1.8\,R*$ that is the energy level decreases. However, for $\omega_c > \geq 1.8\,R*$ the p effect is higher than γ and the energy increases.

The variation of magnetization as a function of ω_c for different cases of T, p and γ is plotted in Figure 4. The magnetization M has a peak structure and it sign is negative for the derivative of $\langle E\rangle$ with respect to ω_c, This magnetization behaviour can be understood from the average energy plot shown in Figure 3(a). At low magnetic field, the energy decreases (negative slope) and at a minimum point ($B \sim .5$ T), the energy starts increasing (positive slope), which leads to the flipping in the sign of the magnetization $\left(M = -\frac{\Delta E}{\Delta B}\right)$ as the slope of the magnetization of the average energy–magnetic field (E–B) curve, from positive to negative, while the magnetic susceptibility $\left(\chi = \frac{\Delta M}{\Delta B}\right)$ in this case changes it sign from positive (paramagnetic) to negative (diamagnetic) QD-material.

At $p = 1$ and $\gamma = 0a^*.R^*$, we show in in Figure 4(a), the effect of changing γ on the $M - \omega_c - plot$. We see that M increases until $\omega_c \approx 0.8R^*$ for $T = 5$ K and then decreases, but it is decreasing when the temperature is increasing. However, in Figure 4(b) for $\gamma = 0.7a^*.R^*$, the magnetization, M, decreases with increasing ω_c while M decreases as increases T at constant ω_c. In Figures 4(c,d), we show the effect of Rashba effect, for $p = 1.5$, on the M-magnetic field curve. For example, Figure 4(c) shows that magnetization, M decreases, as shown in Figure 4(c).

Furthermore, in Figure 4(d), when $\gamma = 0.7a^*.R^*$ and $p = 1.5$ it decreases faster for all ω_c. On the other hand, M decreases for $\gamma = .7a^*.R^*$, displayed in Figure 4(d).

The variation of the susceptibility as a function of ω_c for various values of T, p and γ is shown in Figure 5, where χ is the derivative of M with respect to B. We can see from the Figure 5(a) that at $p = 1$ and $\gamma = 0a^*.R^*$, the magnetic susceptibility for T = 5 and 10 K is positive ($\chi > 0$) until $\omega_c \approx 0.8\,R^*$ and then it changes to negative ($\chi < 0$). This sign flipping in χ means that the material can change its type from diamagnetic to paramagnetic. In Figure 5(b) with Rashba coupling ($\gamma = 0.7a^*.R^*$) the material is diamagnetic for different temperature. When $p = 1.5$ in Figure 5(c), χ is negative for all ω_c range at $T = 10$, 20 and 30 K, while its positive

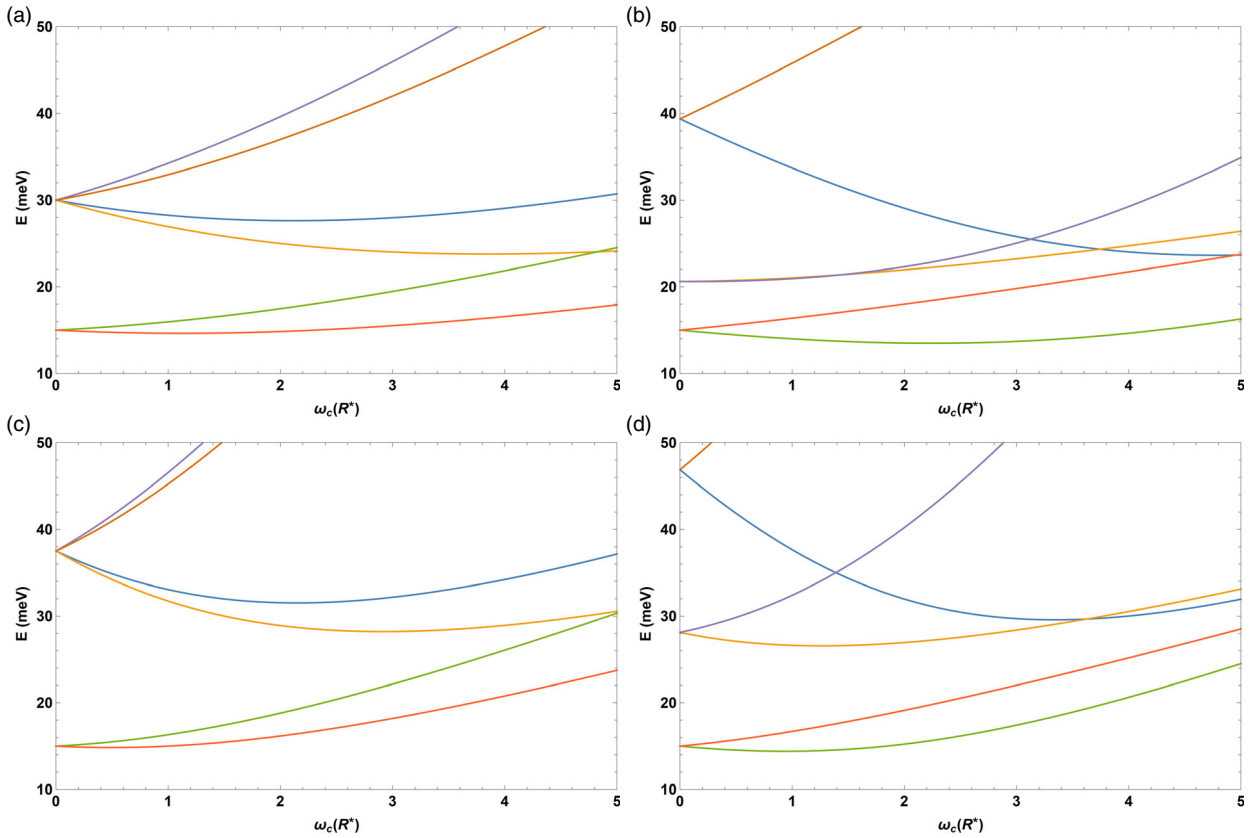

Figure 2. Energy spectra for the ground state ($n = 0$) as a function of the magnetic field with $\omega_0 = 2.5\ R*$ for (a) $p = 1, \gamma = 0$ (b) $p = 1, \gamma = 0.5\ a^*R^*$ (c) $p = 1.5, \gamma = 0$, and (d) $p = 1.5, \gamma = 0.5a^*R^*$.

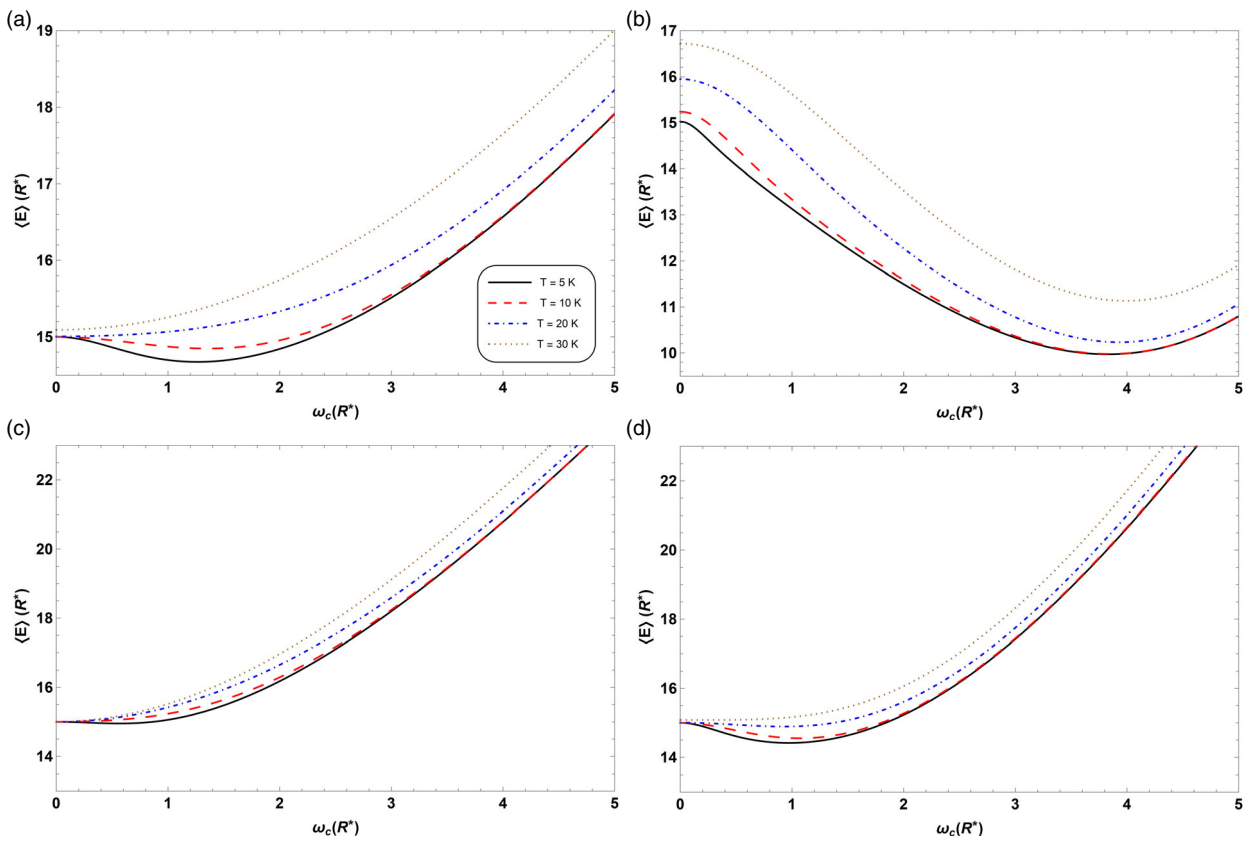

Figure 3. Statistical average energy as a function of the magnetic field with $\omega_0 = 2.5\ R*$ and different temperature (solid line T = 5 K, dashed line T = 10 K, dotted dashed line T = 20 K and double dotted dashed line T = 30 K) for (a) $p = 1, \gamma = 0$ (b) $p = 1, \gamma = 0.5\ a^*R^*$ (c) $p = 1.5, \gamma = 0$ and (d) $p = 1.5, \gamma = 0.5\ a^*R^*$.

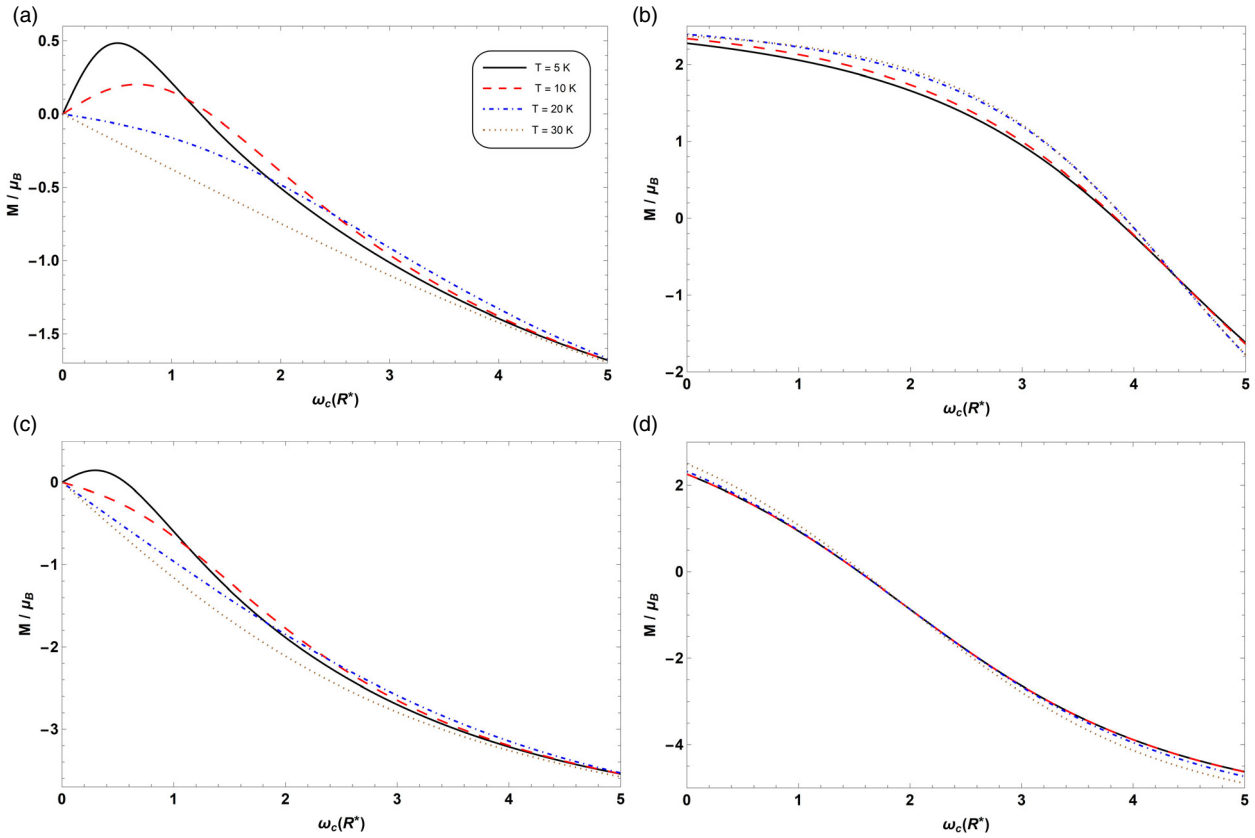

Figure 4. Magnetization as a function of the magnetic field with $\omega_0 = 2.5\,R^*$ and different temperature (solid line $T = 5$ K, dashed line T = 10 K, dotted dashed line $T = 20$ K and double dotted dashed line $T = 30$ K) for (a) $p = 1$, $\gamma = 0$ (b) $p = 1$, $\gamma = 0.5\,a^*R^*$ (c) $p = 1.5$, $\gamma = 0$ and (d) $p = 1.5$, $\gamma = 0.5\,a^*R^*$.

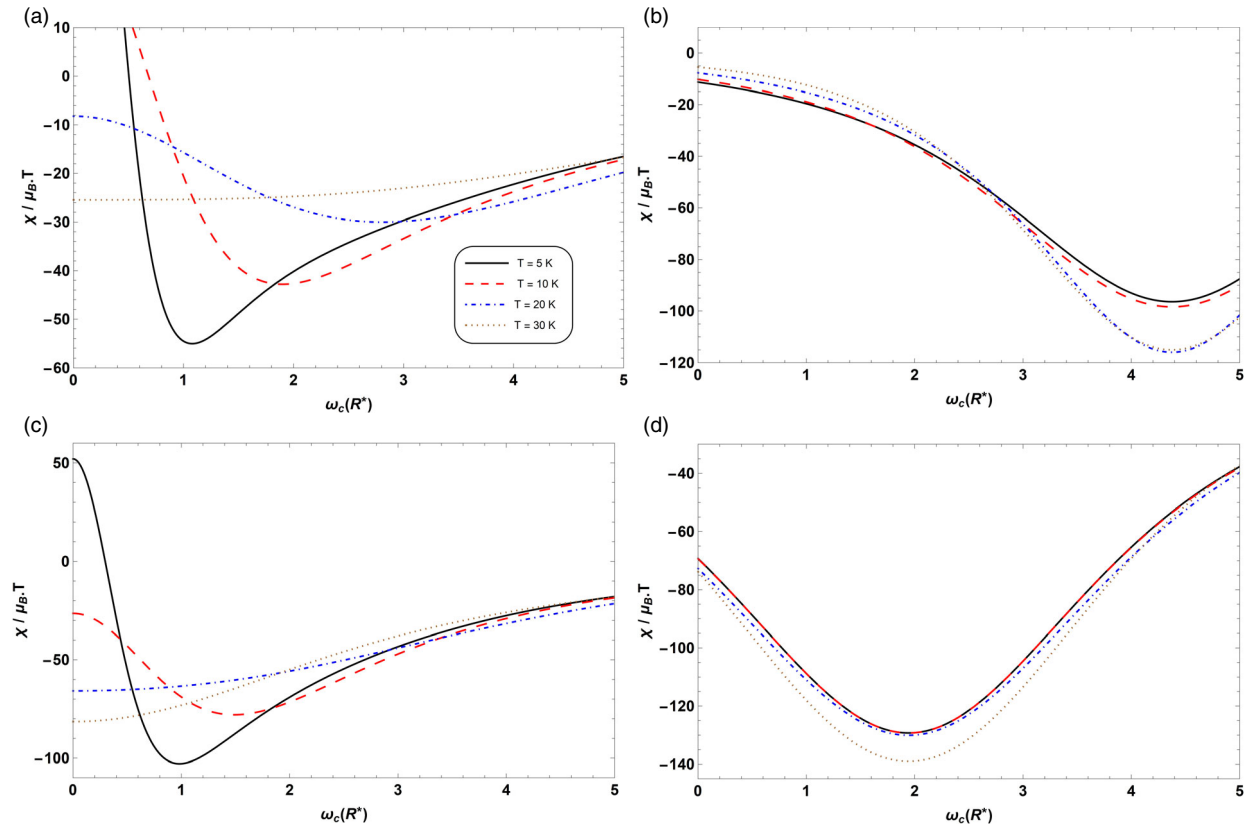

Figure 5. Magnetic susceptibility as a function of the magnetic field with $\omega_0 = 2.5\,R^*$ and different temperature (solid line $T = 5$ K, dashed line $T = 10$ K, dotted dashed line $T = 20$ K and double dotted dashed line $T = 30$ K) for (a) $p = 1$, $\gamma = 0$ (b) $p = 1$, $\gamma = 0.5\,a^*R^*$ (c) $p = 1.5$, $\gamma = 0$ and (d) $p = 1.5$, $\gamma = 0.5\,a^*R^*$.

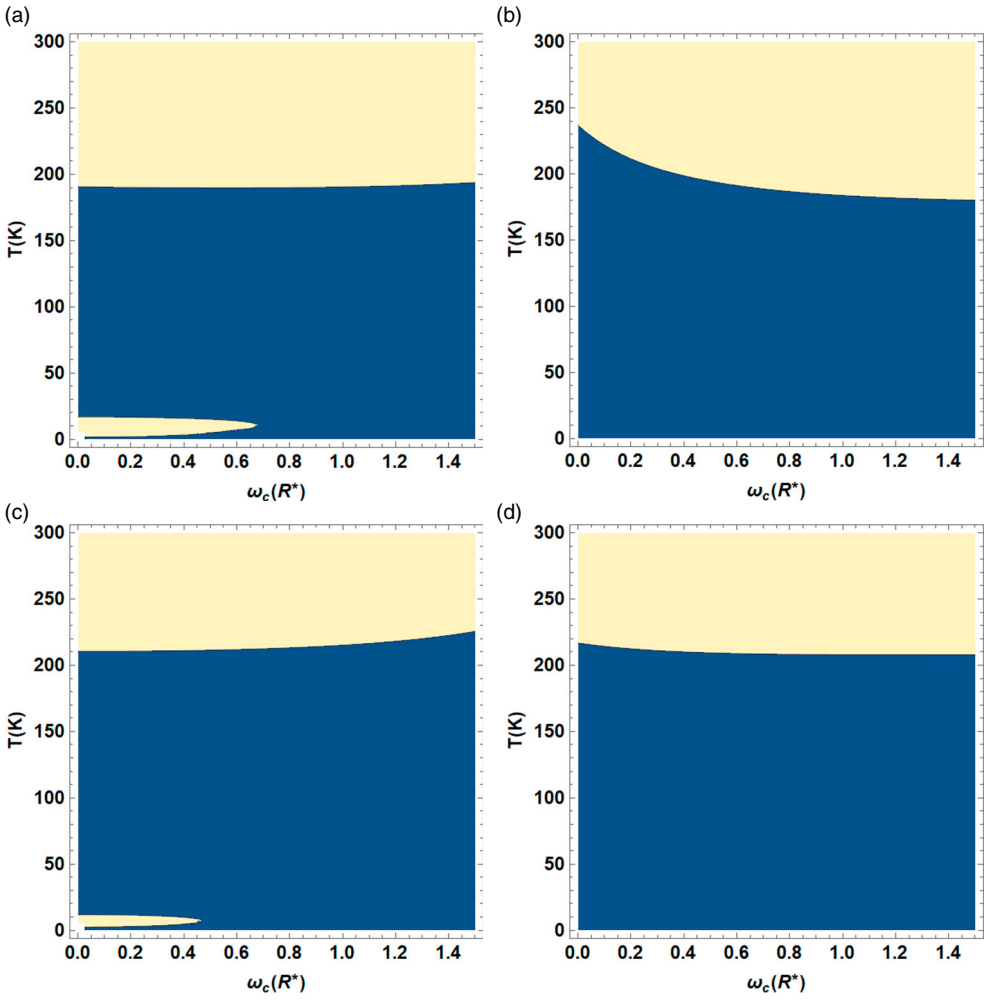

Figure 6. Magnetic phase diagram of GaAs QD as a function of the T and ω_C with $\omega_0 = 2.5R*$ for (a) $p = 1, \gamma = 0\, a*.R*$, (b) $p = 1$, $\gamma = 0.35\, a*.R*$, (C) $p = 1.2, \gamma = 0\, a*.R*$ and (b) $p = 1.2$ and $\gamma = 0.35\, a*.R*$. The golden region corresponds to the paramagnetic phase ($\chi > 0$) whereas the blue region to the diamagnetic phase ($\chi < 0$).

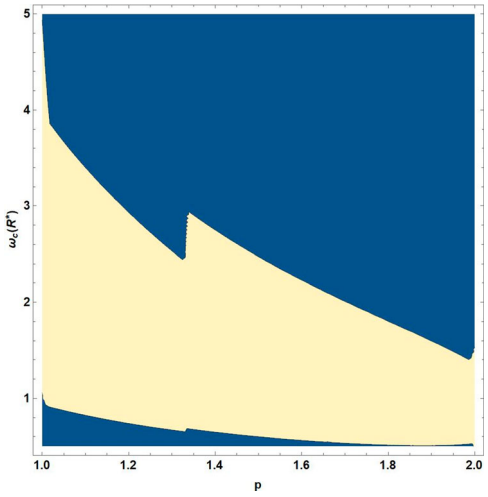

Figure 7. Magnetic phase diagram of GaAs diagram QD as a function of ω_c and large range of topological defect (p), from $p = 1$ to $p = 2$, with $\omega_0 = 0.5R^*$, .

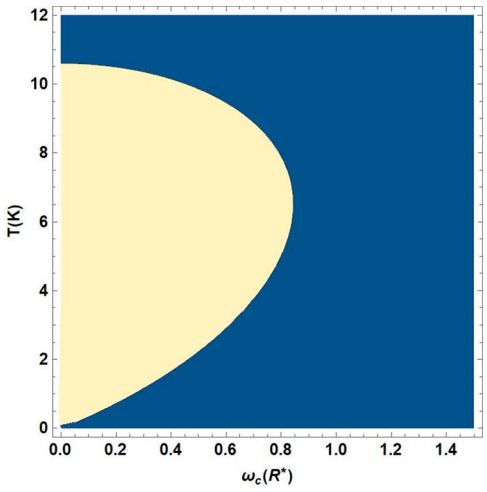

Figure 8. Computed magnetic phase diagram of GaAs QD ($p = 1, \gamma = 0, \omega_0 = 6.3R^*$) as a function of T and ω_C which corresponding one given by Ref. [17].

until $\omega_c = 0.4\ R^*$ and then negative at $T = 5$ K, with both Rashba and topological effects as in Figure 5(d), the effect of Rashba is higher and χ is negative for various ω_c and T.

We search for the magnetic phase diagrams of the GaAs nanomaterial for a wide range of QD physical parameters. To achieve our objective, we present

a contour-plot (Figures 6(a–d) for the magnetic susceptibility of the QD as function of the QD-physical parameters.

Figure 6(a) shows the phase transition obtained by equation (12), without any external affect. The obtained contour plot, for various QD-parameters, is in a very good agreement with the corresponding one given by Refs. [11,17]. To investigate further the effects of topological defect, we have presented additional contour plot, Figure 7, for a wide range of defect parameter ($p = 1.0–2.0$), small confinement ($\omega_0 = 0.5R^*$) and quite high temperature ($T \approx 250K$). The figure shows obviously the roles of topological functions: p, T and ω_0 in controlling the magnetic type transition of the QD-material from diamagnetic ($\chi < 0$) to paramagnetic ($\chi > 0$) phase diagrams. Furthermore, the present magnetic susceptibility contour plot shown in Figure 8, and for $p = 1$ case, is compared, against the corresponding one shown in Ref. [17], where the authors had obtained the contour plot of the magnetic susceptibility by approximating the gaussian QD model (GQD) as a parabolic type confining potential, in terms of gaussian confining potential strength, V_0, and QD radius, R, *as* $\omega_h^2 = \frac{V_0}{m^* R^2}$.

4. Conclusion

In this work, the Hamiltonian of a single electron confined in a parabolic QD including various external factors like: Rashba spin orbit interaction term effect, applied uniform magnetic field and topological defect had been used in a closed form. We have studied the dependence of the energy spectra for our QD as a function of: confinement frequency (ω_0), magnetic field (ω_c), Rashba (γ) and topological defect (p). Our energy results obtained from a close energy expression are in very good agreement with reported works [15]. The computed results show that if we increase the topological factor (p), the $\langle E \rangle$ increases also and this result affects significantly M and χ of the QD-material. The behaviour of the magnetic susceptibility χ is shown against the QD functions. We found that the QD material changes its magnetic phase from diamagnetic ($\chi < 0$) to paramagnetic ($\chi > 0$) type [13]. These magnetic transition phase diagrams of the QD are shown explicitly in the contour plots as function of various physical functions of the QD-Hamiltonian.

Disclosure statement

No potential conflict of interest was reported by the author(s).

ORCID

Nouf Ibrahim http://orcid.org/0000-0002-0081-005X
Muayad Abu Saa http://orcid.org/0000-0002-1443-1501
Ayham Shaer http://orcid.org/0000-0002-6518-6470
Mohammad Elsaid http://orcid.org/0000-0002-1392-3192

References

[1] Shah SH. Study of nonlinear optical properties of indium arsenide/gallium arsenide and indium gallium arsenide/gallium arsenide self-assembled quantum dots. Delaware: University of Delaware; 2007.
[2] Ashoori RC. Electrons in artificial atoms. Nature. 1996; 379(6564):413–419.
[3] Harrison P, Valavanis A. Quantum wells, wires and dots: theoretical and computational physics of semiconductor nanostructures: Hoboken, NJ: John Wiley & Sons; 2016.
[4] Christians JA, Fung RC, Kamat PV. An inorganic hole conductor for organo-lead halide perovskite solar cells. improved hole conductivity with copper iodide. J Am Chem Soc. 2014;136(2):758–764.
[5] Jamieson T, Bakhshi R, Petrova D, et al. Biological applications of quantum dots. Biomaterials. 2007;28(31): 4717–4732.
[6] Reshma VG, Mohanan PV. Quantum dots: applications and safety consequences. J Lumin. 2019;205: 287–298.
[7] Baghdasaryan DA, Hayrapetyan DB, Kazaryan EM, et al. Thermal and magnetic properties of electron gas in toroidal quantum. Physica E. 2018;101:1–4.
[8] Nammas FS. Thermodynamic properties of two electrons quantum dot with harmonic interaction. Physica A. 2018;508:187–198.
[9] Sedeh HRR, Khordad R. Magnetocaloric effect, magnetic susceptibility and specific heat of tuned quantum dot/ring system. Physica E. 2021;134:114884.
[10] Edet CO, Ikot AN, Onyeaju MC, et al. Thermo-magnetic properties of the screened Kratzer potential with spatially varying mass under the influence of Aharanov–Bohm (AB) and position-dependent magnetic fields. Physica E. 2021;131:114710.
[11] Antil S, Kumar M, Lahon S, et al. Pressure dependent optical properties of quantum dot with spin orbit interaction and magnetic field. Optik (Stuttg). 2019;176: 278–286.
[12] Sari H, Kasapoglu E, Sakiroglu S, et al. Impurity-related optical response in a 2D and 3D quantum dot with Gaussian confinement under intense laser field. Philos Mag. 2020;100(5):619–641.
[13] Kumar DS, Mukhopadhyay S, Chatterjee A. Magnetization and susceptibility of a parabolic in as quantum dot with electron–electron and spin–orbit interactions in the presence of a magnetic field at finite temperature. J Magn Magn Mater. 2016;418:169–174.
[14] Avetisyan S, Pietiläinen P, Chakraborty T. Strong enhancement of Rashba spin-orbit coupling with increasing anisotropy in the Fock-Darwin states of a quantum. Phys Rev B. 2012;85(15):153301.
[15] Castano-Yepes JD, Amor-Quiroz DA, Ramirez-Gutierrez CF, et al. Impact of a topological defect and Rashba spin-orbit interaction on the thermo-magnetic and optical properties of a 2D semiconductor quantum dot with Gaussian confinement. Physica E. 2019;109: 59–66.
[16] Shaer A, Elsaid MK, Elhasan M. Magnetization of GaAs parabolic quantum dot by variation method. J Phys Sci Appl. 2016;6(2):39–46.
[17] Boyacioglu B, Chatterjee A. Dia-and paramagnetism and total susceptibility of GaAs quantum dots with Gaussian confinement. Physica E. 2012;44(9):1826–1831.